

## Supporting Information

### Atomic Thin NiB<sub>6</sub> Monolayer: A Robust Dirac Material

Xiao Tang,<sup>a</sup> Weiguo Sun,<sup>b</sup> Cheng Lu,<sup>\*c</sup> Liangzhi Kou<sup>\*a</sup> and Changfeng Chen<sup>\*c</sup>

<sup>a</sup> School of Chemistry, Physics and Mechanical Engineering, Queensland University of Technology, Gardens Point Campus, Brisbane, QLD 4001, Australia

<sup>b</sup> Institute of Atomic and Molecular Physics, Sichuan University, Chengdu 610065, China

<sup>c</sup> Department of Physics and Astronomy, University of Nevada, Las Vegas, Nevada 89154, USA

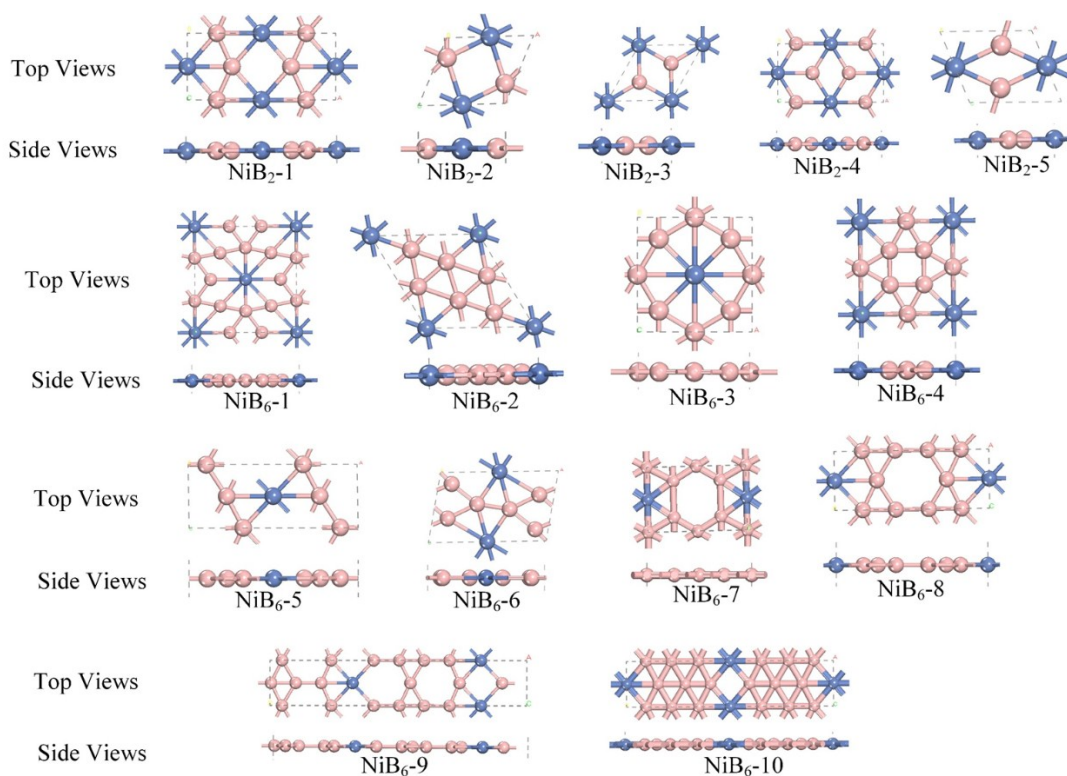


**Fig. S1:** Monolayer Ni<sub>x</sub>B<sub>y</sub> structures searched from CALYPSO code, which are however not stable as checked from phonon calculations.

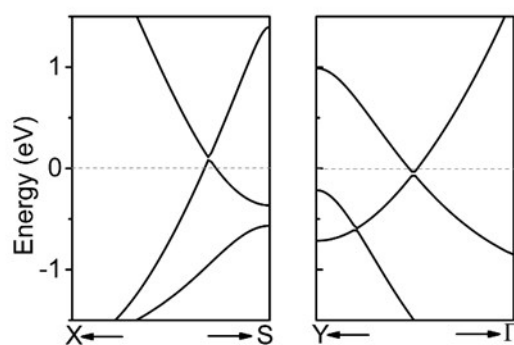


**Fig. S2** Dirac cone 1 (left panel) and cone 2 (right panel) of the NiB<sub>6</sub> monolayer calculated using the HSE06 functional. The Fermi level is set to zero.

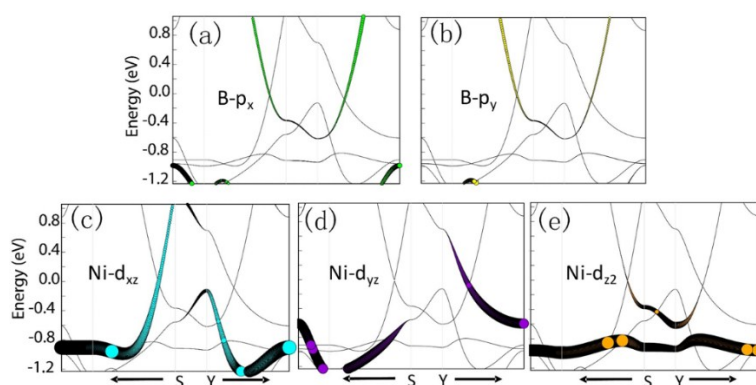


**Fig. S3** Orbital-resolved band structures of the NiB<sub>6</sub> monolayer contributed by (a)  $p_x$ , (b)  $p_y$  from the B atoms and (c)  $d_{xz}$ , (d)  $d_{yz}$ , and (e)  $d_{z^2}$  from the Ni atoms. The size of the circles represent the level of contribution. The Fermi level is set to zero.

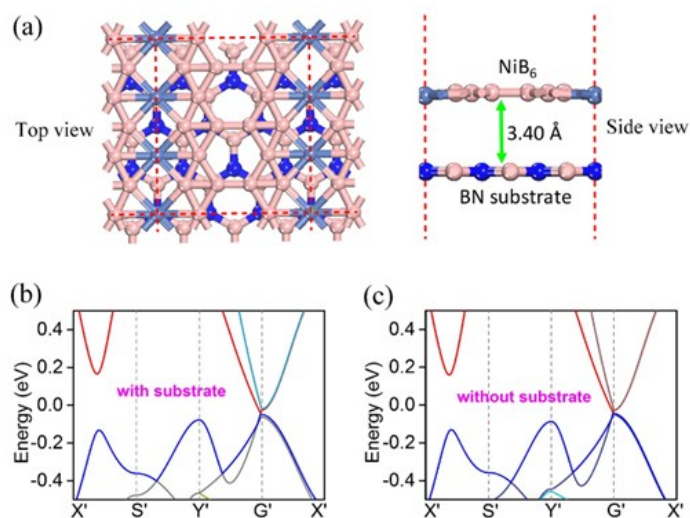


**Fig. S4** (a) Top view and side view of optimized NiB<sub>6</sub> with BN substrate. Band structures of NiB<sub>6</sub> monolayer (b) with (c) without BN substrate. The Fermi level is set to zero.

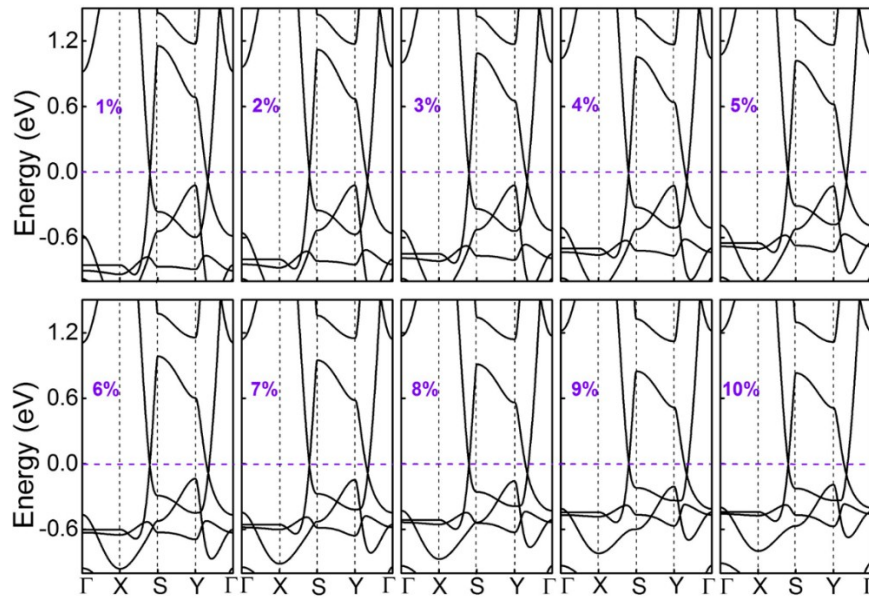


**Fig. S5** Band structures under a biaxial strain (*a* and *b* directions). The Fermi level is set to zero.

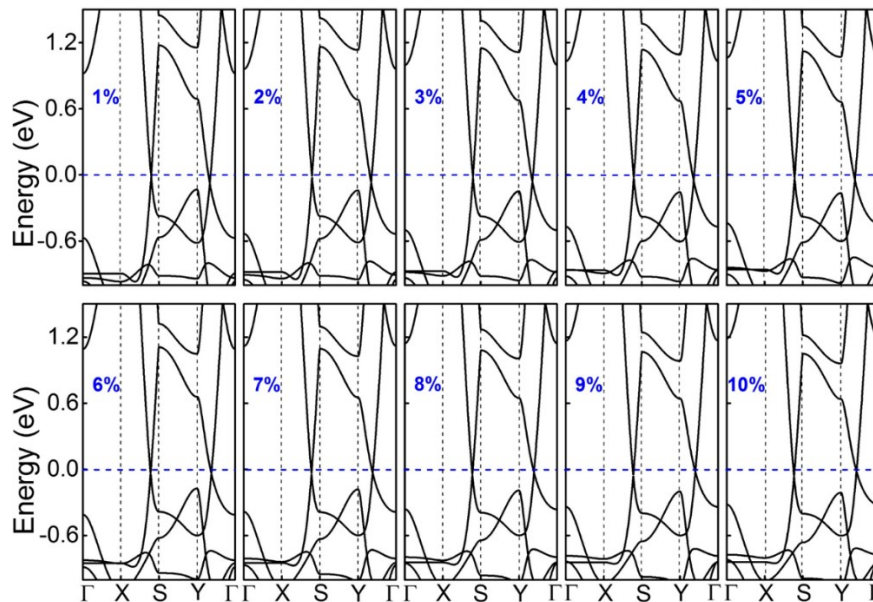


**Fig. S6** Band structures under a uniaxial strain (*a* direction). The Fermi level is set to zero.

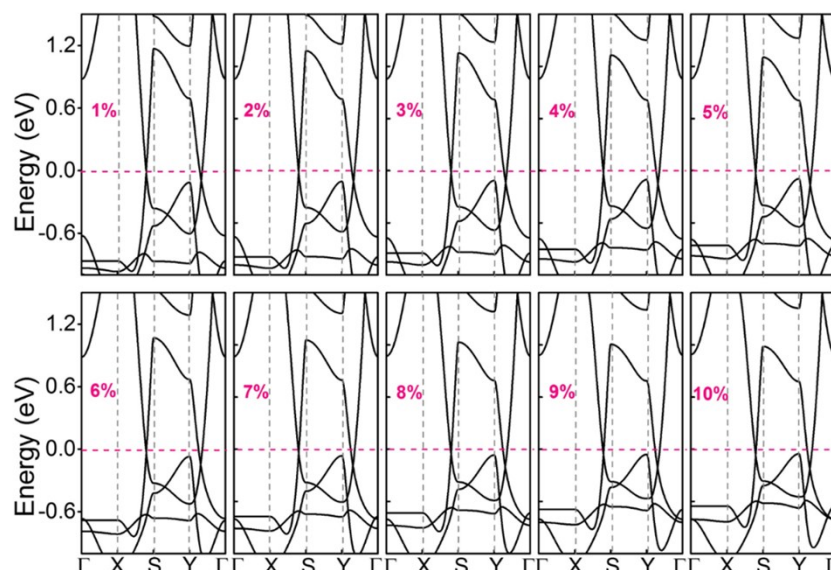


**Fig. S7** Band structures under a uniaxial strain (*b* direction). The Fermi level is set to zero.

Detailed results from an adaptive natural density partitioning analysis are shown in Fig. S8. The first chemical bond depicts the long pairs of the  $d_{xz}$  orbital of the vertex Ni atom with  $ON = 1.991 |e|$ , compared to  $2.00 |e|$  in the ideal case. Eight 2c-2e Ni-B  $\sigma$  bonds with  $ON = 1.991 |e|$  and  $1.985 |e|$  indicate the interactions among the vertex Ni and neighboring B atoms. The additional localized 2c-2e  $\sigma$  bonds ( $ON = 1.901 |e|$ ) is shown by two bridge B atoms between the two  $Ni_2B_4$  molecular configurations. The peripheral vertex Ni atoms contribute to the Ni-B  $\sigma$  delocalized bonds and form four 3c-2e  $\sigma$  bonds with  $ON = 1.978 |e|$ . In the  $Ni_2B_4$  molecule, the interaction between the two vertex Ni atoms and central B atom contribute to two 3c-2e  $\sigma$  bonds ( $ON = 1.936 |e|$ ), while the other four 3c-2e  $\sigma$  bonds are formed by three B atoms with  $ON = 1.882 |e|$ . Two delocalized  $\pi$  bonds among the four B atoms in each  $Ni_2B_4$  molecule contribute to the 4c-2e  $\pi$  bonds ( $ON = 1.924 |e|$ ). The last two 5c-2e bonds describe the  $\sigma$  bonds with a low occupation number of  $ON = 1.907 |e|$ , which are mainly contributed by the 3d orbital of the Ni atom. Thus, the 2c-2e and 3c-2e  $\sigma$  bonds contribute to the substantial stability of the quasi-planar  $Ni_4B_8^+$  molecular.

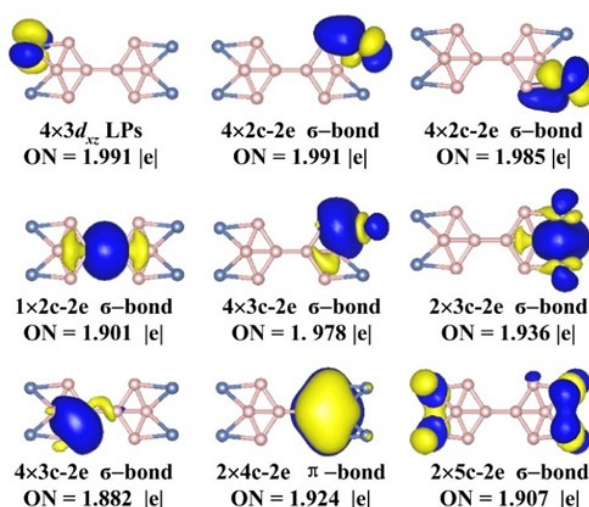


**Fig. S8** A chemical bonding analysis of the  $Ni_4B_8^+$  molecule. ON stands for the occupation number.

